A&A 417, 807–817 (2004)
DOI: 10.1051/0004-6361:20040018

Astronomy & Astrophysics

Cosmic ray acceleration by spiral shocks in the galactic wind

H. J. Völk[1] and V. N. Zirakashvili[2]

[1] Max-Planck-Institut für Kernphysik, 69029, Heidelberg, Postfach 103980, Germany
e-mail: Heinrich.Voelk@mpi-hd.mpg.de
[2] Institute for Terrestrial Magnetism, Ionosphere and Radiowave Propagation, 142190, Troitsk, Moscow Region, Russia

Received 17 March 2003 / Accepted 15 January 2004

Abstract. Cosmic ray acceleration by shocks related with Slipping Interaction Regions (SIRs) in the Galactic Wind is considered. SIRs are similar to Solar Wind Corotating Interaction Regions. The spiral structure of our Galaxy results in a strong nonuniformity of the Galactic Wind flow and in SIR formation at distances of 50 to 100 kpc. SIRs are not corotating with the gas and magnetic field because the angular velocity of the spiral pattern differs from that of the Galactic rotation. It is shown that the collective reacceleration of the cosmic ray particles with charge Ze in the resulting shock ensemble can explain the observable cosmic ray spectrum beyond the "knee" up to energies of the order of $10^{17}\,Z$ eV. For the reaccelerated particles the Galactic Wind termination shock acts as a reflecting boundary.

Key words. ISM: cosmic rays – acceleration of particules

1. Introduction

The hypothesis that the origin of the cosmic rays (CRs) is predominantly the result of diffusive shock acceleration at the blast waves of individual supernova remnants (SNRs) has the corollary (e.g. Lagage & Cesarsky 1983; Völk 1987; Axford 1994) that this mechanism should only work up to particle rigidities (energy per charge) that are a decade below the so-called knee of the spectrum at rigidities around several 10^{15} Volts, or somewhat more. The only consistent way to escape this conclusion is to assume that the magnetic field strength at these shocks substantially exceeds the typical interstellar values of several μG. Such high field configurations might be unusually strong stellar fields in the winds of very massive stars (Berezinsky & Ptuskin 1988; Völk & Biermann 1988; Biermann 1993), or the strong Alfvénic wave turbulence excited at strong shock waves, as speculated by Völk (1984) and recently calculated in a simplified nonlinear model by Lucek & Bell (2000) and Bell & Lucek (2001). However, also this field amplification is limited and for a SN explosion into an essentially uniform external medium (SNe type Ia and core collapse SNe from stars of zero age main sequence masses below about 15 $M_\odot$ which have little main sequence mass loss) knee energies constitute a firm upper bound (Völk et al. 2002). Our working hypothesis is therefore that the knee corresponds to the cutoff for the CR sources in the disk. Regarding core collapse SN explosions into the winds of massive progenitor stars on the other hand, Bell & Lucek (2001) have even pondered the possibility for an extension of the SNR origin of CRs to energies far above the knee, up to 10^{18} eV for protons and to $10^{18}\,Z$ eV for heavy nuclei. The observed steepening of the all-particle energy spectrum – and presumably also of the energy spectra of individual nuclei (Kampert et al. 2001) – above the knee at 3×10^{15} Volt they attributed somewhat vaguely to source statistics. Whether such a picture of disk sources, with single power law spectra reaching beyond the knee up to rigidities of about 10^{17} Volt, is consistent with the rigidity dependence of the escape from the Galaxy, is an open question. In any case no one of the very optimistic SNR scenarios aims at an explanation of the all-particle spectrum beyond 3×10^{18} eV, the so-called ankle, where the spectrum appears to harden again (for a recent summary, see Sommers 2001). And these ultra-high energy CRs are not our concern here either. They may be extragalactic or due to a top-down mechanism of the decay of hypothetical superheavy particles left over from the early Universe (for a review see Bhattacharjee & Sigl 2000).

Assuming from now on that the CR sources in the disk cut off at the knee, we propose here a rather different mechanism to accelerate CRs in the Galaxy to energies between the knee and the ankle. This mechanism remains nevertheless intimately connected with the mechanical energy input from stars into the interstellar medium in the form of winds and SN explosions. For the process to operate we start from the assumption that the Galaxy exhibits a significant supersonic mass loss. It is mainly driven by the CRs and the hot gas generated in the disk, and removes about 1 $M_\odot\,\mathrm{yr}^{-1}$ from the Galaxy with a terminal speed of several 100 $\mathrm{km\,s}^{-1}$ that is of the order of the escape velocity (Ipavich 1975; Breitschwerdt et al. 1991, 1993; Zirakashvili et al. 1996; Ptuskin et al. 1997). Such a *Galactic Wind* must develop because these CRs are tightly coupled to the thermal

Send offprint requests to: V. N. Zirakashvili,
e-mail: Zirak@izmiran.rssi.ru

gas and the magnetic field of the interstellar medium and therefore tend to establish an essentially infinite scale height above the disk due to their ultrarelativistic mean energy. The coupling is due to scattering on magnetic fluctuations which the escaping particles excite themselves in the low-density halo of the Galaxy. Supersonic speeds are eventually reached at distances of about 20 kpc corresponding to the size of the disk.

The new aspect which we emphasize here is based on the consideration that even on a large scale this outflow must be far from regular in space and time, and that its variations should be of the same order as the mean. We shall argue that due to the rotation of the Galaxy the differences in flow speed will lead to strong internal wind compressions, bounded by *smooth* CR shocks in an expanding halo gas whose internal energy density is dominated by that of the CRs from the disk. These CR shocks *reaccelerate* the most energetic particles produced in the disk by about 2 orders of magnitude in rigidity. The re-acceleration essentially ensures the continuity of the energy spectrum at the knee. A fraction of the re-accelerated particles will return to the disk, filling a very thick (several tens of kpc) region including the Galactic mid-plane rather *uniformly and isotropically*. Since at these energies the propagation in the average wind environment is diffusive (Ptuskin et al. 1997), also their spatial density in the disk is about equal to that of the knee particles. We shall call the reaccelerated particles here "Wind-CRs", and the primary CRs from compact regions in the disk we shall call "Disk-CRs", for obvious reasons. These names indicate the origin of the particles which is not only different in time but also in space.

Galactic reacceleration mechanisms have been frequently considered in the past. This concerned reacceleration of CRs by shocks in the Galactic disk (e.g. Blandford & Ostriker 1980; Berezhko & Krymsky 1983; Bykov & Toptygin 1988; Ip & Axford 1991; Klepach et al. 2000), or acceleration of particles at the termination shock of the Galactic Wind (Jokipii & Morfill 1985, 1987).

Reacceleration in the Galactic disk can not give large enough energies of accelerated particles because the size and life time of the shocks are quite limited. A different case is the acceleration at the Galactic Wind termination shock which can be steady state and is very extended (about several hundred kpc). The investigation of acceleration on such a shock results in rather large maximum energies of the accelerated particles of about 10^{17} to 10^{18} eV for CR protons (Jokipii & Morfill 1987) On the other hand, this form of reacceleration faces the difficulty of the observation of these particles in the disk. The matter is that the condition of efficient acceleration at the termination shock coincides with the condition for strong modulation of particles inside the Galactic Wind flow. For a diffusion coefficient which increases with energy only the highest energy particles accelerated at the termination shock can be observed near Earth.

The alternative source of shocks in the Galactic Wind flow which we have indicated above are interaction regions far above the rotating disk. They are somewhat similar to the so-called Corotating Interaction Regions in the Solar Wind (Fig. 1), although the differences in their characteristics are quite important. Galactic interaction regions are due to the

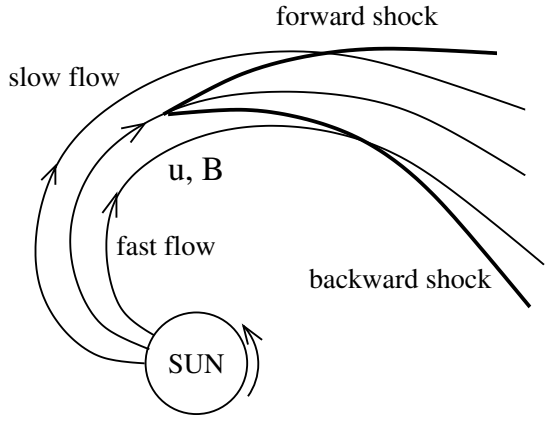

Fig. 1. Schematic picture of a Corotation Interaction Region in the Solar Wind. The fast stream flows into the interaction region through the backward shock, whereas the slow stream enters the interaction region through the forward shock. Magnetic field and plasma velocity are parallel in the reference frame rotating with the Sun.

fact that much of the high-mass star formation in the Galaxy and the associated active regions such as superbubbles and OB-associations, including most of the SNRs, is concentrated in the spiral arms. These rotate relative to the gas in a quasi-stationary pattern with a related mechanical energy input from stellar winds and SN explosions that implies an enhanced wind in terms of an increased mass velocity (see also Breitschwerdt et al. 2002). In the Parker spiral-type magnetic field structure (Parker 1958) that the outflow from a magnetized Galactic disk generates (Zirakashvili et al. 1996), faster wind streams from more active regions will begin to overtake slower streams after the wind has formed in the upper halo. If the relative flow speed is supersonic, the interaction will lead to a shock pair like in the Solar Wind. As long as the flow speed of the wind is still low for a given rotation rate of the wind source region, quasi-periodic compression regions will form that lead only to a series of forward shocks after a steepening time, interleaved with rarefaction waves. This distinct situation applies to the Galaxy, as we shall see. Indeed, the flow time to the sonic point, from a reference level ∼1 kpc above the disk midplane where the smooth wind flow hydrodynamics is already a good approximation, is larger than or comparable with the Galactic rotation time. In this sense the Galaxy is a fast rotator whereas the Sun is a slow rotator: the wind flow time from the base of the corona to the sonic point is short compared to the solar rotation time. A second difference is given by the fact that the magnetic field lines are rooted in the gas of the disk, especially in the massive molecular clouds, rather than in its spiral pattern, and are therefore only temporarily compressed in the spiral arms. The angular velocity of the interaction regions equals the spiral pattern angular velocity and the angular velocity of frozen-in magnetic field lines equals the Galactic angular velocity.

As a result, the interaction regions propagate as a wave phenomenon across the magnetic flux tubes. From the point of view of the interaction regions the magnetic field lines slip through them. That is why we shall rather call these interaction regions Slipping Interaction Regions (SIRs). This slip also means that particles that were accelerated at one of the shocks

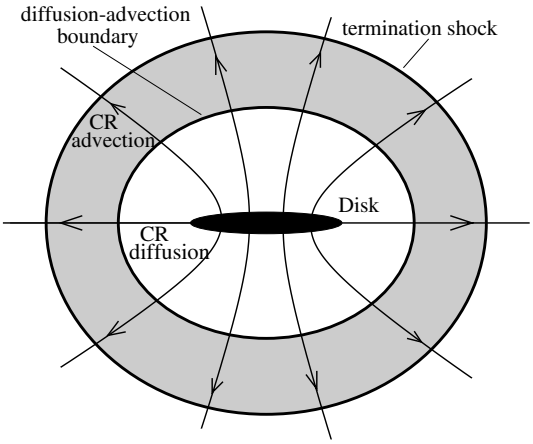

Fig. 2. Meridional cross-section of the Galactic Wind flow. The direction of the gas velocity is shown by the arrows. The supersonic gas flow is bounded by the termination shock. CR transport is mainly diffusive inside the diffusion-advection boundary; outside this boundary it is determined by convection in the gas flow (in the dashed region). The galactic disk is indicated by the black ellipse.

will be able to leave the shock region eventually to escape along a field line, rather than only across the field like in the Corotating Interaction Regions of the Solar Wind. To this extent the acceleration properties of the rotating Galactic halo are quite different from those of the Corotating Interaction Regions of the Solar Wind discussed many years ago by Fisk & Lee (1980).

In this paper we shall consider reacceleration of Disk-CRs by SIR shocks in the Galactic Wind flow, the large scale propagation of the high energy Wind-CRs in the wind-disk regions, and the resulting anisotropies. The paper is organized as follows: brief descriptions of CR transport and of the Galactic Wind flow are given in Sects. 2 and 3, respectively. Numerical calculations of SIR shock formation are presented in Sect. 4. CR reacceleration by shocks related with the Galactic spiral structure is introduced in Sect. 5 and calculated in Sect. 6. Section 7 contains the conclusions.

2. Cosmic ray propagation in the Galactic Wind flow

A schematic picture of the Galactic Wind flow geometry is given in Fig. 2. The azimuthally symmetric flow originates in the Galactic disk and extends the frozen-in magnetic field. At small heights above the disk the gas velocity is perpendicular to the galactic disk. The flow is approximately radial at large distances from the Galaxy. The gas is assumed to be fully ionized in the wind, supporting magnetohydrodynamic waves. These may also be resonantly excited by the anisotropic streaming of the CR component. Their amplitudes will ultimately be limited by damping through nonlinear wave-particle interactions.

A complete and self-consistent model of CR propagation in such a flow has been considered by Ptuskin et al. (1997). The CR diffusion coefficient is determined by Alfvén waves generated by the CR streaming instability. CRs produced in the disk – the Disk-CRs – diffuse along magnetic field lines. This diffusion flux generates Alfvén waves and they propagate in the Galactic Wind flow. The generation of Alfvén waves is balanced by nonlinear Landau damping. The resulting diffusion coefficient $D_{\parallel}^{s}$ along the magnetic field does not depend on distance and is approximately given by

$$D_{\parallel}^{s} \simeq 10^{27}(p/m_{\rm p}c)^{\gamma_{\rm d}-3}\ {\rm cm}^2\ {\rm s}^{-1}. \quad (1)$$

Here p is momentum of the particle, $m_{\rm p}$ is the proton mass and $\gamma_{\rm d}$ is the power law index of the momentum distribution of the CR sources in the disk; its numerical value is close to 4. The CR spectrum near in and near to the Galactic disk is formed as the result of the interplay between diffusion and advection. At small distances from Galactic midplane diffusion dominates advection. At large distances diffusion is weaker because the gradient scale increases and because the magnetic field becomes rather azimuthal. Diffusion and advection are comparable at some distance $R_{\rm da}$. This distance increases with particle momentum as $p^{(\gamma_{\rm d}-3)/3}$. For the diffusion coefficient given by Eq. (1) and a wind velocity $u = 300\ {\rm km\,s^{-1}}$, $R_{\rm da}(1\ {\rm TeV}) \approx 15$ kpc, approximately equal to the disk radius.

The supersonic Galactic Wind flow is bounded by a termination shock at some distance $R_{\rm s}$ from the Galaxy. This distance depends on the intergalactic pressure which is poorly known. Estimates give a value of several hundred kpc. One has to expect that the termination shock creates strong MHD turbulence downstream, towards intergalactic space. CR diffusion is strongly reduced in this case and should be close to the Bohm limit. For those CRs whose propagation characteristics in the Galactic Wind (inside the termination shock) are diffusive, the termination shock can therefore be considered as a reflecting boundary. This holds up to a maximum particle rigidity that is determined by the condition $D_{\rm B} \sim uR_{\rm s}$ where $D_{\rm B} = vr_{\rm g}/3$ is the Bohm diffusion coefficient of particles with gyroradius $r_{\rm g}$ and velocity v. Its numerical value is determined by the local magnetic field strength. At large distances in the then spherically symmetric Galactic Wind flow the magnetic field strength is given by:

$$B \approx B_{\rm g}\frac{R_{\rm g}^2\Omega(\theta)\sin\theta}{Ru}, \quad (2)$$

where θ denotes Galactic colatitude, $B_{\rm g}$ is the poloidal field strength in the disk, $R_{\rm g}$ is the Galactic radius and Ω is the angular velocity of Galactic rotation. Then, using Eq. (2), the above estimate $D_{\rm B} \sim uR_{\rm s}$ gives the following maximum energy

$$E_{\rm max} = Z\sin\theta\left(\frac{\Omega(\theta)}{10^{-15}\ {\rm s^{-1}}}\right)\left(\frac{B_{\rm g}}{2\,\mu{\rm G}}\right)\cdot\left(\frac{R_{\rm g}}{15\ {\rm kpc}}\right)^2 1.2\times10^{17}\ {\rm eV}, \quad (3)$$

where Z is the nuclear charge number of the particle. We should note that this energy is not small for small θ because the angular velocity of the galactic rotation Ω increases toward the galactic center. Higher energy particles cross the termination shock diffusively.

2.1. Single power law sources up to E_{max} in the disk?

Let us assume now that the sources in the Galactic disk produce CRs with a single power law spectrum up to very high rigidities. If the rigidity of the particles is small enough so that

the distance to the diffusion-advection boundary $R_{\rm da}(p) < R_{\rm s}$ then in the Galactic disk the spectrum of such Disk-CRs will be modified relative to the source spectrum proportional to $p^{-\gamma_{\rm d}} R_{\rm da}^{-2}(p)$. This happens as long as $E < E_*$, where E_* is given by $R_{\rm da}(E_*) = R_{\rm s}$ and corresponds to $E_* \sim 10^{16}\, Z$ eV for $R_{\rm s} = 300$ kpc. Particles with larger rigidities freely diffuse in the space interior to the termination shock and can only escape convectively through this shock in an energy independent manner because of the small diffusion coefficient beyond. Hence the observed spectrum must be the same as the source spectrum. As a result we should observe a hardening of the spectrum in the energy range $E_* < E < E_{\rm max}$ (see Appendix A for an approximate analytical calculation of this effect).

However, this spectral hardening is not observed. We therefore conclude that Galactic sources must have a cut-off energy smaller than E_* which in turn is essentially equal to the knee energy $E_{\rm knee} \simeq 3 \times 10^{15}$ eV. As a consequence the notion of a single power law source spectrum, produced in the Galactic disk, must be ruled out. Its basis was the somewhat arbitrary assumption that Galactic escape might become even more effective beyond the knee (e.g. Hillas 1984). In the light of a consistent physical model for the overall CR transport in the Galaxy this hypothesis is untenable. We rather believe that reacceleration in the Galactic Wind inside the termination shock should produce particles with energies $E_{\rm knee} < E < E_{\rm max}$ with the same source spectrum as the spectrum observed in the disk. In a bottom-up scenario of acceleration from lower energies, higher energy particles should mainly come from beyond the termination shock.

2.2. Quantitative definition of Disk-CRs vs. Wind-CRs

We can now make our qualitative definitions of Disk-CRs and Wind-CRs from the Introduction more precise: equating $E_{\rm knee} = E_*$ the Disk-CRs are those energetic particles with $E < E_{\rm knee}$, and their sources are in the disk; Wind-CRs are the particles with $E_{\rm knee} < E < E_{\rm max}$ whose source is of a quasi-diffuse nature in the Galactic Wind.

3. Spiral structure of our Galaxy, wind shocks

The spiral pattern of late-type galaxies was explained theoretically by Lin & Shu (1964) as a density wave in the distribution of stars in the disk of galaxies. It is believed now that our Galaxy possesses a two or four spiral arm structure, or even a mixed two-four arm spiral pattern (Lépine et al. 2001). This pattern rotates rigidly with angular velocity $\Omega_{\rm p}$. Therefore the dependence of the wave amplitude on time t and azimuthal angle φ is given by $\exp(im(\varphi - \Omega_{\rm p} t))$, where m is the number of spiral arms. The estimates for the angular velocity of the spiral pattern are very uncertain and controversial. The old value is $\Omega_{\rm p} = 13.5$ km s^{-1} kpc^{-1} (Lin et al. 1969). Lépine & Amaral (1997) found $\Omega_{\rm p} = 20$ km s^{-1} kpc^{-1}, Lépin et al. (2001) argue in favor of $\Omega_{\rm p} = 26$ km s^{-1} kpc^{-1}. On the other hand Fernandez et al. (2001) give the value $\Omega_{\rm p} = 30$ km s^{-1} kpc^{-1}. In any case, the Sun is not located far from the corotation radius at which the Galactic rotation velocity equals the pattern velocity. The rotation velocity of the Galaxy at the Sun's position is approximately $\Omega = 26$ km s^{-1} kpc^{-1}.

Since potential CR sources in the disk are primarily concentrated in the spiral arms, we can assume that the CR pressure in and above the spiral arms is larger than between the arms. Hence, the CR-driven Galactic Wind flow should be modulated by the spiral structure. The situation differs from the Solar Wind case because of the relatively fast rotation of the Galaxy. Indeed, the Galactic Wind flow time to the (magneto)sonic point is about 100 million years and is comparable with the period of Galactic rotation. This means that the modulation by the spiral pattern should produce magnetosonic waves, propagating in the Galactic Wind flow. At large distance from the Galaxy these spiral compression waves propagate in the radial direction and approximately perpendicular to the wind magnetic field which is by then practically azimuthal. The radial and azimuthal wavenumbers for these waves are:

$$k_r = \frac{\Omega_{\rm p} m}{u_{\rm s}}, k_\phi = \frac{m}{r}, \tag{4}$$

where $u_{\rm s}$ the radial velocity of the wave. This value is approximately the sum of the wind velocity u and the phase velocity of the fast magnetosonic waves $c_{\rm f}$ traveling in the radial direction. At large distances we simply have

$$c_{\rm f} = \sqrt{V_{\rm a}^2 + c_{\rm s}^2}$$

where $V_{\rm a}$ and $c_{\rm s}$ are the Alfvén and the sound velocity, respectively.

The nonlinear steepening of magnetosonic waves can produce a train of forward shocks at large Galactocentric distances. The characteristic distance can be found from the following estimate. The inverse steepening time is $k_r \delta u$, where δu is the velocity perturbation in the wave. During this time the wave propagates the distance $\delta r \sim (u + c_{\rm f})/(k_r \delta u)$. Using the expression for the radial wave number we obtain:

$$\delta r \sim \frac{(u + c_{\rm f})^2}{m \Omega_{\rm p} \delta u}.$$

For $u + c_{\rm f} \sim 400$ km s^{-1}, $\delta u \sim 50$ km s^{-1}, and $m = 2$, δr is about 60 kpc. The velocity perturbation δu is half of the velocity jump at the shock formed. We therefore conclude that spiral shock formation is possible at distances of 60 to 100 kpc. Numerical results (see below) confirm this estimate. These spiral shocks should not be confused with the spiral density wave in the Galactic disk. The radial dependence of the spiral density wave in the Galactic disk will be transformed into a latitude dependence of the spiral shocks in the Galactic Wind flow (see Fig. 2).

We should underline that the shocks in the Galactic Wind have two distinct features in comparison with the Solar Wind.

First of all the shock structure is stationary in the frame of reference corotating with the spiral pattern. Material Galactic rotation still exists in this frame except at special Galactocentric radii. Therefore these shocks are not in corotation with the matter in the Galactic disk but rather slip through it and this is why we shall call them SIR shocks. Such a particular feature can be very important for diffusive shock acceleration of particles. This can be appreciated by comparing the

Galaxy with the Sun. It is simple to see that the particles accelerated in the shocks of Corotating Interaction Regions of the Solar Wind are drawn into the Corotating Interaction Region between the forward and backward shocks (see Fig. 1). In addition, energetic particles diffuse predominantly along magnetic lines which are immobile in the frame corotating with the Sun. Hence, particles that are moving backward to the Sun should pass through the shock again, which is difficult because of the small diffusion coefficient generated near the shock and in the downstream region of the gas flow. Therefore it is only possible to observe these particles in the space between the Sun and the Interaction Region (e.g. in the neighborhood of the Earth) if they diffuse across the field which is a very slow process. Galactic SIR shocks, on the other hand, are not in corotation with the wind magnetic field lines because these field lines are anchored in the Interstellar gas of the Galactic disk. Hence the inner parts of field lines become "free" towards the disk (after the shock has left them behind and the shock-created turbulence has subsided). This allows SIR-accelerated particles to reach the disk along magnetic field lines without any necessity to invoke perpendicular diffusion.

The second feature is the absence of backward SIR shocks. Outward moving large-amplitude periodic waves steepen into a train of shocks (saw-tooth wave), where forward shocks are followed by rarefaction waves, like in a gas at rest.

4. Numerical calculations of SIR shocks

In this section we present numerical calculations of SIR shock formation in the Galactic Wind flow. We shall use a simplified spherical geometry for the Galactic Wind flow and investigate the formation of SIR shocks propagating in the Galactic equatorial plane. For simplicity we describe thermal gas and CRs in a two-fluid approximation with two-dimensional magnetohydrodynamic equations including CRs (see, e.g., Zirakashvili et al. 1996):

$$\frac{\partial \rho}{\partial t} = -\frac{1}{r^2}\frac{\partial}{\partial r}\left(r^2 u\rho\right) - \frac{1}{r}\frac{\partial}{\partial \varphi}\left(u_\varphi \rho\right) \tag{5}$$

$$\frac{\partial u}{\partial t} = -u\frac{\partial u}{\partial r} - \frac{u_\varphi}{r}\frac{\partial u}{\partial \varphi} + \frac{u_\varphi^2}{r} - \frac{\partial \Phi}{\partial r} - \frac{1}{\rho}\frac{\partial}{\partial r}\left(P_\mathrm{c} + P_\mathrm{g} + \frac{B_\varphi^2}{8\pi}\right) + \frac{1}{4\pi\rho}\left(\frac{B_\varphi}{r}\frac{\partial B}{\partial \varphi} - \frac{B_\varphi^2}{r}\right) \tag{6}$$

$$\frac{\partial u_\varphi}{\partial t} = -u\frac{\partial u_\varphi}{\partial r} - \frac{u_\varphi}{r}\frac{\partial u_\varphi}{\partial \varphi} - \frac{u_\varphi u}{r} - \frac{1}{\rho r}\frac{\partial}{\partial \varphi}\left(P_\mathrm{c} + P_\mathrm{g} + \frac{B^2}{8\pi}\right) + \frac{1}{4\pi\rho}\left(B\frac{\partial B_\varphi}{\partial r} + \frac{B_\varphi B}{r}\right) \tag{7}$$

$$\frac{\partial B_\varphi}{\partial t} = -u\frac{\partial B_\varphi}{\partial r} - \frac{u_\varphi}{r}\frac{\partial B_\varphi}{\partial \varphi} + Br\frac{\partial}{\partial r}\frac{u_\varphi}{r} - \frac{B_\varphi}{r}\frac{\partial}{\partial r}(ru) \tag{8}$$

$$\frac{1}{r}\frac{\partial B_\varphi}{\partial \varphi} + \frac{1}{r^2}\frac{\partial}{\partial r}\left(r^2 B\right) = 0 \tag{9}$$

$$\frac{\partial P_\mathrm{g}}{\partial t} = -u\frac{\partial P_\mathrm{g}}{\partial r} - \frac{u_\varphi}{r}\frac{\partial P_\mathrm{g}}{\partial \varphi} - \gamma_\mathrm{g} P_\mathrm{g}\left(\frac{1}{r^2}\frac{\partial}{\partial r}\left(r^2 u\right) + \frac{1}{r}\frac{\partial u_\varphi}{\partial \varphi}\right) - \left(\gamma_\mathrm{g} - 1\right)\left(v_\mathrm{a}\frac{\partial P_\mathrm{c}}{\partial r} + v_{\mathrm{a}\varphi}\frac{\partial P_\mathrm{c}}{\partial \varphi}\right) \tag{10}$$

$$\frac{\partial P_\mathrm{c}}{\partial t} = -(u + v_\mathrm{a})\frac{\partial P_\mathrm{c}}{\partial r} - \frac{u_\varphi + v_{\mathrm{a}\varphi}}{r}\frac{\partial P_\mathrm{c}}{\partial \varphi} - \gamma_\mathrm{c} P_\mathrm{c}\left(\frac{1}{r^2}\frac{\partial}{\partial r}\left(r^2(u + v_\mathrm{a})\right) + \frac{1}{r}\frac{\partial}{\partial \varphi}(u_\varphi + v_{\mathrm{a}\varphi})\right). \tag{11}$$

Here ρ is the gas density, u and B denote the radial components of the gas velocity and the magnetic field respectively, u_φ and B_φ are the azimuthal components of the gas velocity and the magnetic field, Φ is the gravitational potential, P_g and P_c are the gas and CR pressures, respectively, γ_g and γ_c with $\gamma_\mathrm{c} < \gamma_\mathrm{g}$ are the adiabatic indices of the thermal gas and the CR gas, and $v_\mathrm{a} = B/\sqrt{4\pi\rho}$ and $v_{\mathrm{a}\varphi} = B_\varphi/\sqrt{4\pi\rho}$ are the radial and azimuthal components of the Alfvén velocity, respectively.

Equation (5) describes mass conservation. The overall momentum balance Eqs. (6) and (7) determine the mass motion in the radial and azimuthal directions. Equations (8) and (9) describe the evolution of the frozen-in magnetic field. The time evolution of the CR pressure is given by Eq. (11), neglecting diffusion in the frame of the waves. This is an excellent approximation for the description of these large-scale structures since the CR pressure is mainly determined by low-energy CR particles produced in the Galactic Disk. The transport of these particles is completely dominated by advection in the SIR waves. Following Zirakashvili et al. (1996) we assume that CR streaming generates Alfvén waves propagating along the magnetic field out of the Galaxy. These waves are damped and heat the gas. This dissipative effect is described by the last term in the equation for the gas pressure, Eq. (10).

The gravitational potential Φ was chosen in the following simplified, spherically symmetric form:

$$\Phi = \Phi_0 - \frac{GM_\mathrm{B,D}}{r} + \frac{GM_\mathrm{H}}{R_\mathrm{H}}\ln\left(1 + \frac{r}{R_\mathrm{H}}\right) \tag{12}$$

for $r < 100$ kpc. Here $G = 6.668 \times 10^{-8}$ cm^3 g^{-1} s^{-2} denotes the gravitational constant. The second term on the rhs describes the gravitational potential of the Galactic disk and bulge, and the third term is the potential of the Dark Matter Halo with radius 100 kpc. We used the values $M_\mathrm{B,D} = 9.97 \times 10^{10}\ M_\odot$, $M_\mathrm{H} = 1.07 \times 10^{11}\ M_\odot$, $R_\mathrm{H} = 12$ kpc from Allen & Santillán (1991). The total mass of the Dark Matter Halo amounts to $8.0 \times 10^{11}\ M_\odot$.

The system of Eqs. (5) to (11) was solved numerically using an explicit finite-difference scheme. Artificial viscosity was included to avoid numerical instabilities. At the base level at $r = 15$ kpc we fixed the gas number density $n_0 = 0.001$ cm^{-3}, the radial magnetic field component $B_0 = 1.0 \times 10^{-6}$ G, the gas temperature $T = 7.25 \times 10^5$ K, and the azimuthal velocity $u_{\varphi 0} = 220$ km s^{-1}. Adiabatic indices $\gamma_\mathrm{g} = 5/3$ and $\gamma_\mathrm{c} = 4/3$ were used. The CR energy flux $F_\mathrm{c} = \gamma_\mathrm{c}(u + v_\mathrm{a})P_\mathrm{c}/(\gamma_\mathrm{c} - 1)$, modulated by the spiral structure, was taken in the form

$$F_\mathrm{c} = F_{\mathrm{c}0}\left(1 + 0.5\sin(m(\varphi - \Omega_\mathrm{p} t))\right) \tag{13}$$

which assumes that the power of the Disk-CR sources in the spiral arms is a factor of three larger than between the arms. For the numerical calculations we used $m = 2$, $\Omega_\mathrm{p} = 30$ km s^{-1} kpc^{-1} and $F_{\mathrm{c}0} = 2.0 \times 10^{-5}$ erg cm^{-2} s^{-1}.

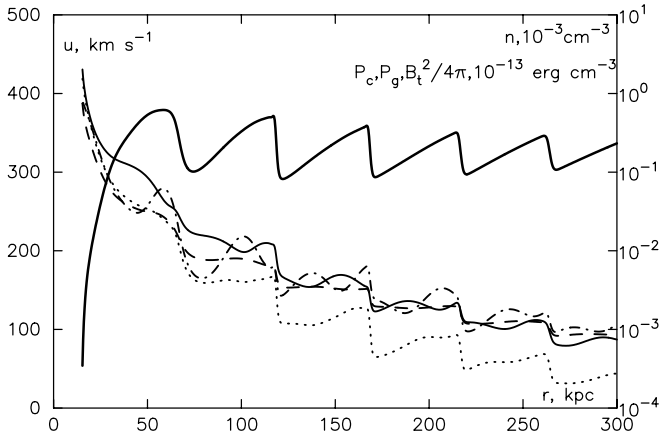

Fig. 3. Radial dependencies, taken at one azimuth angle. The values of the radial gas velocity u (thick solid line, in units of km s^{-1}) are given on the left abscissa. The right abscissa shows the values of the cosmic ray and gas pressures P_c (thing solid line) and P_g (dotted line), respectively (in units of 10^{-13} erg cm^{-3}), the gas number density n (dashed line, in units of 10^{-3}cm^{-3}), and the total magnetic field tension $B_t^2/4\pi$ (dash-dotted line, in units of 10^{-13} erg cm^{-3}). Forward SIR shocks form a saw-tooth velocity profile at large distances in the Galactic Wind flow.

Numerical results are shown in Fig. 3. One can see that SIR shocks with a velocity jump of the order 100 km s^{-1} are formed at distances exceeding 50 kpc. These SIR shocks form a saw-tooth wave velocity profile. The compression ratio σ_s of these shocks is about 2.0. In the sequel we shall call the entire saw-tooth wave the "SIR shock system".

We emphasize that our numerical results show the presence of forward shocks only. Backward shocks were also observed at initial times in the computation. Nevertheless the backward shocks were blown out at large times when all quantities depend on r and $\varphi - \Omega_p t$ only. A similar result was obtained by Cranmer & Owocki (1996) for the formation of Corotating Interaction Regions in O-star winds.

5. Reacceleration of particles by the SIR shock system: Physics conditions

We shall consider now the possibilities for standard diffusive shock wave acceleration in the spiral SIR shock system. A similar consideration was made by Spruit (1988) for spiral accretion shocks. Due to the fact that the wind is primarily driven by the CRs which have a softer equation of state and dominate the thermal part of the pressure (Zirakashvili et al. 1996), Galactic Wind SIR shocks are basically smoothed by the pressure of the "low" energy Disk-CRs (compare Drury & Völk 1981); in addition, they are almost perpendicular shocks. In this case there is *no injection of particles from the thermal pool* and SIR shocks will only *reaccelerate* Disk-CRs with energies E close to E_{knee} to energies beyond the knee.

It is interesting to consider the implications of this situation. First of all, the SIR shock system will not modify the spectral form of the Disk-CRs below the knee. Since the average adiabatic compression in the saw-tooth wave is zero, there will also be no net adiabatic number or energy density increase of the Disk-CRs; the spectrum is still determined by the interplay of the sources in the disk and the propagation in the wind. Secondly, the energy requirements for the production of the Wind-CRs by the SIR shock system are minimal because no other particles are energized in the process. The total escape energy loss of the Wind-CRs is given by their convective energy flow through a spherical surface at the radial position of the termination shock (see below).

The magnetic field in the Galactic Wind is rather strong. As a result, the Mach number of the wind flow is not very large. We expect that SIR shocks are not very strong either and that the spectrum of the particles accelerated by a single shock of the SIR shock system will be fairly steep. On the other hand, particles with energies of the Wind-CRs are diffusively locked inside the termination shock and can be continuously reaccelerated by the system of SIR shocks. It is well known that in such a situation the spectrum of accelerated particles can be harder than that due to a single shock (e.g. Blandford & Ostriker 1980; Spruit 1988; Achterberg 1990; Melrose & Pope 1993; Klepach et al. 2000). The only caveat here is that all those many-shock acceleration theories were based on the test particle approximation in a system of shocks with a strictly discontinuous velocity profile. We shall also follow this approach here, even though the finite width of the actual SIR shocks should not only produce a power law distribution of Wind-CRs but at the same time prevent any increase of the Disk-CRs.

The Parker spiral angle α between the magnetic field and the radial direction is given by the expression

$$\cos\alpha = \frac{u}{\sqrt{\Omega^2 r^2 \sin^2\theta + u^2}}. \qquad (14)$$

We shall assume that the Galactic Wind flow is bounded by a strong termination shock at distance R_s, where the wind velocity drops by a factor σ, the shock compression ratio. Beyond the termination shock the gas flow is subsonic and is dynamically dominated by the sum of gas, magnetic, and CR pressures. One may assume that the Galactic Wind flow is highly turbulent in this downstream region. We shall assume that for all particles of Galactic origin, Disk-CRs and Wind-CRs, diffusion is negligible in comparison with advection beyond the termination shock.

The scattering of the energetic particles is weaker interior to the termination shock. Nevertheless, as already mentioned in the Introduction, particles with $E < E_{max}$ can be accelerated at the termination shock if the diffusion coefficient is small enough there. They can not be observed inside the Galaxy for the same reason. Very high energy particles, with $E > E_{max}$ and a correspondingly high diffusion coefficient, coming from the termination shock or beyond, can be observed in the disk, but can not be accelerated at the termination shock.

We proceed now to the calculation of the reacceleration of Disk-CRs by the SIR shock system with spatial period $L = 2\pi/k_r$ and velocity jump Δu. The condition for efficient diffusive shock wave acceleration is $D \lesssim (u_s - u)L/6$, where D is the diffusion coefficient in the direction of the shock normal. It means that the diffusion time $(Dk_r^2)^{-1}$ must be large in comparison with the advection time $(k_r(u_s - u))^{-1}$. In the Bohm limit

this condition gives a maximum energy of accelerated particles that is smaller than the maximum energy given by Eq. (3). However, the SIR shocks are almost perpendicular and therefore the diffusion coefficient in the direction of the shock normal can be smaller than the Bohm value if the shock-associated turbulence is moderate. This implies a larger maximum energy than that corresponding to the Bohm limit. A necessary condition for this situation to apply is $D_{\parallel}/D_{\rm B} < v/u_{\rm s}$ (Jokipii 1987). For our parameters this condition is fulfilled within a large dynamic range. However expression (3) still gives the maximum energy for collective reacceleration, because at larger energies the particles leave across the terminal shock rather than remaining confined in the reacceleration region. Perpendicular collisionless shocks with Mach numbers smaller than 2 should have a laminar structure (cf. Sagdeev 1966; Forslund & Freiberg 1971). Therefore a moderate level of MHD turbulence downstream of the individual SIR shocks and small CR diffusion coefficients in the direction of the shock normals are possible. Drift motions in the inhomogeneous regular magnetic field in the latitudinal direction can also diminish the maximum energy of accelerated particles since the SIR shock system depends on latitude. However, we expect the regular magnetic field to be small because the regular poloidal magnetic field component is weak in our Galaxy (cf. Han & Qiao 1994). Galactic Wind streams originating from different parts of the Galactic disk should drag out random magnetic field and magnetic loops with sizes of the order of 1 kpc. These magnetic disturbances become strongly elongated at large distances from the Galaxy due to the acceleration and spherical expansion of the Galactic Wind flow (cf. Zirakashvili et al. 2001). Hence, the distant wind is filled by almost azimuthal, sign-dependent magnetic fields. But Parker's formula (14) and similar expressions for the magnetic field strength remain valid for this case as well. CR diffusion in such a field should be very anisotropic. Random drift motions and wandering of magnetic field lines would produce an anomalous transport across magnetic lines.

In the following we shall concentrate on the problems of continuity of the spectrum of the reaccelerated particles and of the possibility to observe them in the Galaxy. For the sake of simplicity we shall neglect anomalous perpendicular transport and treat CR diffusion as one-dimensional similar to the paper of Fisk & Lee (1980).

Let us calculate the angle between the magnetic field and the shock normal $\alpha_{\rm s}$. Using (4) and (14) we obtain for $r \gg u/\Omega$

$$\cos\alpha_{\rm s} = \left(\frac{\Omega u_{\rm s}}{\Omega_{\rm p} u} - 1\right)\cos\alpha. \tag{15}$$

One can easily see that this can be zero for a Galactic Wind flow line originating at a particular galactocentric radius, which means that the corresponding SIR shocks are purely perpendicular shocks. The acceleration by these shocks will be efficient if $D_{\parallel}\cos^2\alpha_{\rm s} \lesssim (u_{\rm s}-u)L/6$. On the other hand, particles accelerated near the termination shock can be observed in the Galaxy if $D_{\parallel}\cos^2\alpha \gtrsim uR_{\rm s}$. These two inequalities can coexist only in the case

$$\left(\frac{\Omega u_{\rm s}}{\Omega_{\rm p} u} - 1\right)^2 < \frac{(u_{\rm s}-u)L}{6uR_{\rm s}} = \frac{\pi(u_{\rm s}-u)u_{\rm s}}{3mu\Omega_{\rm p}R_{\rm s}}. \tag{16}$$

This condition determines the part of the Galactic Wind flow filled by effectively accelerating SIR shocks which produce CRs that are observable in the Galactic disk. They are the Wind-CRs.

6. Acceleration of the Wind-CRs

For the sake of simplicity we shall consider CR propagation in the Galactic Wind equatorial plane. The evolution of the isotropic part of the CR momentum distribution function $N(r,t,p)$ inside the termination shock $r < R_{\rm s}$ is given by

$$\begin{aligned}\frac{\partial N}{\partial t} &= \frac{1}{r^2}\frac{\partial}{\partial r}r^2 D_{\parallel}\cos^2\alpha\frac{\partial N}{\partial r} - u\frac{\partial N}{\partial r}\\ &+\frac{2up}{3r}\frac{\partial N}{\partial p} + Q(p)\frac{\delta(r-r_0)}{4\pi r_0^2}\\ &+\frac{\Delta u}{L}\left(\frac{p}{3}\frac{\partial N}{\partial p} - \frac{1}{\ln\sigma_{\rm s}}\int_0^p\frac{dp'}{p'}\left(\frac{p'}{p}\right)^{\gamma_{\rm s}}\frac{N(p')-N(p)}{\ln(p'/p)}\right).\end{aligned} \tag{17}$$

Here p is the momentum of the particle, $D_{\parallel}$ is the cosmic ray diffusion coefficient along the magnetic field, α is the angle between the magnetic field and the radial direction, u is the Galactic Wind velocity, and $Q(p)$ describes the source of CR particles at the radial distance $r_0 = 15$ kpc from the galactic centre. The CR distribution function N is normalized as $n = 4\pi\int p^2 {\rm d}pN$, where n is the CR number density. The last term on the rhs of Eq. (17) describes the collective acceleration by multiple shocks (see Appendix B for details). It combines the adiabatic energy losses of the particles between the SIR shocks of compression ratio $\sigma_{\rm s}$ with multiple reacceleration at these shock fronts (the first and second terms in the round brackets, respectively).

The boundary condition at the termination shock is given by the continuity of N and of the flux density:

$$D_{\parallel}\cos^2\alpha\left.\frac{\partial N}{\partial r}\right|_{r=R_{\rm s}} + u\left(1-\frac{1}{\sigma}\right)\frac{p}{3}\left.\frac{\partial N}{\partial p}\right|_{r=R_{\rm s}} = 0. \tag{18}$$

Note that the termination shock is a reflecting boundary in so far as the downstream diffusion coefficient is taken to be zero in this equation.

The acceleration efficiency of the shock ensemble does not depend on energy. Since the loss of particles into the downstream region of the termination shock is energy independent also, we expect a power law spectrum of the reaccelerated particles, the Wind-CRs. In order to obtain the corresponding spectral index γ we multiply Eq. (17) by the volume element $4\pi r^2{\rm d}r$ and integrate over r from zero to $R_{\rm s}$. In the steady state, using boundary condition (18) and assuming weak modulation inside the termination shock as well as a power law momentum spectrum for the Wind-CRs, we obtain for the index γ the equation:

$$\gamma\left(1 + \frac{R_{\rm s}\sigma\Delta u}{3Lu}\right) + \frac{R_{\rm s}\sigma\Delta u}{Lu}\frac{\ln(1-\gamma/\gamma_{\rm s})}{\ln\sigma_{\rm s}} = 0. \tag{19}$$

The index γ is always between 3 and the single shock spectral index $\gamma_{\rm s} = 3\sigma_{\rm s}/(\sigma_{\rm s}-1)$. We obtained numerical solutions

of Eq. (17) for the Galactic Wind velocity $u = 300\ \mathrm{km\,s^{-1}}$, $R_\mathrm{s} = 300$ kpc, $\sigma = 3$, $m = 2$, $u_\mathrm{s} = 450\ \mathrm{km\,s^{-1}}$, $\Delta u = 100\ \mathrm{km\,s^{-1}}$, $\Omega_\mathrm{p} = 30\ \mathrm{km\,s^{-1}\ kpc^{-1}}$, $\Omega = 20\ \mathrm{km\,s^{-1}\ kpc^{-1}}$. We also take $\gamma_\mathrm{s} = 6$ which corresponds to the SIR shock compression ratio $\sigma_\mathrm{s} = 2$. These numbers determine the solution $\gamma = 4.9$ of Eq. (19). The wave amplitude approximately corresponds to the numerically obtained value from the last section. If we assume that the Galactic disk rotates with a velocity of 200 $\mathrm{km\,s^{-1}}$, independent of Galactocentric distance, then condition (16) will be satisfied for the Galactic Wind flow that originates between 9 and 11 kpc.

The scattering of the Wind-CRs with energies larger than $10^{16}\,Z$ eV on self-generated Alfvén waves is ineffective, since the mean free path corresponding to the diffusion coefficient (1) is larger than 300 kpc. Higher energy particles can be scattered by elongated magnetic field inhomogeneities in the Galactic Wind flow. The mean free path of these latter particles can be of the order of length scale of these inhomogeneities. To take this effect into account we used the diffusion coefficient

$$D_\parallel = D_\parallel^\mathrm{s} \frac{c\lambda}{3} \Big/ \left(D_\parallel^\mathrm{s} + \frac{c\lambda}{3} \right). \tag{20}$$

For numerical calculations we take the energy independent mean free path $\lambda = 2r$. Also, a spectral index of Disk-CR sources $\gamma_\mathrm{d} = 4.0$ and a self-consistent cosmic ray diffusion coefficient $D_\parallel^\mathrm{s} = 10^{27} p/(m_\mathrm{p} c)\ \mathrm{cm^2\ s^{-1}}$ independent of r were used. These values approximately correspond to those obtained in the self-consistent model of CR propagation in the Galaxy (Ptuskin et al. 1997).

We used the spectrum of Disk-CRs sources $Q(p) \sim p^{-\gamma_\mathrm{d}} \exp(-p/p_\mathrm{max})$. The value of the maximum momentum of Disk-CRs sources p_max was taken as $p_\mathrm{max} = 3 \times 10^6\, m_\mathrm{p} c$.

Numerical results are shown in Figs. 4 and 5. Figure 4 shows the spectral energy distribution (SED) of CR protons at the termination shock (dashed curve) and inside the Galaxy (solid curve), respectively, for the case without reacceleration. Note that the resulting acceleration at the termination shock is weak because of the assumed large diffusion coefficient inside the termination shock. Results taking reacceleration into account are shown in Fig. 5. The high energy power-law tail appears beyond the Disk-CR cut-off. The mismatch of the SED by a factor 3 inside the Galaxy is explained by the modulation of the accelerated particles in the Galactic Wind: the Wind-CRs must diffusively penetrate into the inner wind region against the expanding flow.

We found that the strength of this mismatch depends on the unknown form of the cut-off. This feature is demonstrated in Fig. 6 that compares SED of protons in the Galaxy for exponential cut-off (solid line), sharp cut-off (dotted line) and for the cut-off $\propto \exp(-p^2/p_\mathrm{max}^2)$ (dash-dotted line).

The differential spectral flux calculated for the different cosmic ray nuclei and the corresponding all-particle spectral flux, as well as the experimental all-particle spectrum measured by the KASCADE collaboration (Kampert et al. 2001), are shown in Fig. 7. The KASCADE collaboration has since then presented two additional analyses (Antoni et al. 2002; Roth et al. 2003). For the all-particle spectrum they agree within less than 20 percent with the data shown here.

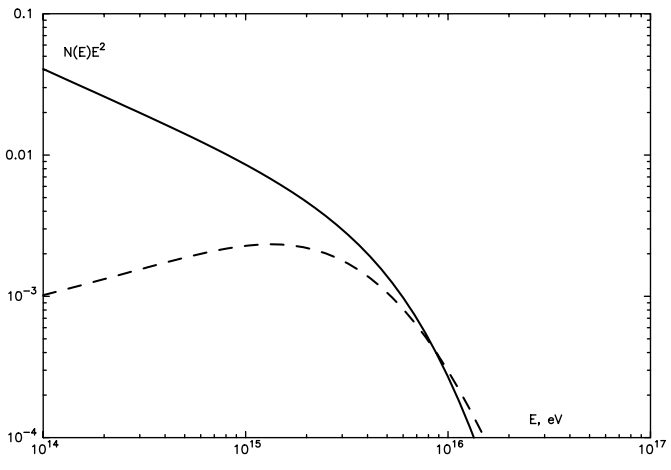

Fig. 4. Spectral energy distributions (in arbitrary units) of the CR protons in the Galaxy (solid curve) and at the termination shock (dashed curve) for the case without reacceleration.

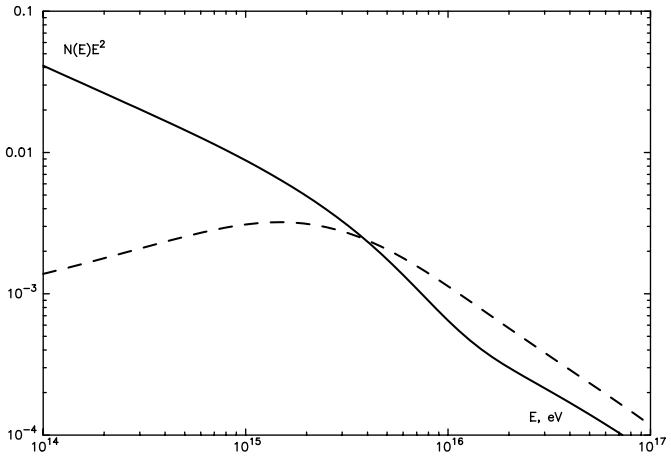

Fig. 5. Spectral energy distributions (in arbitrary units) of the CR protons in the Galaxy (solid curve) and at the termination shock (dashed curve) for the case with reacceleration.

In principle we should use the source power of the Disk CRs as an observational boundary condition in the Galaxy, and then calculate the particle spectrum below the knee. Instead, we have fitted the amplitude of the proton spectrum in Eq. (17) to the observations just below the knee. This fitted proton source power of $7{\times}10^{40}\ \mathrm{erg\,s^{-1}}$ is within 20% the same as that deduced by Ptuskin et al. (1997). To put this number into perspective, we assume an average mechanical energy $E_\mathrm{SN} = 10^{51}$ erg to be released per SN explosion, and a 10 percent average efficiency $\Theta = 10^{-1}$ of conversion of this energy into CR energy. The resulting Galactic Supernova rate is then $\nu_\mathrm{SN} \approx 1/(45\ \mathrm{yr})$.

7. Conclusion

This paper can be considered as an extension of our previous models for the dynamics of the Galactic Wind and for CR propagation in the Galaxy (Breitschwerdt et al. 1991, 1993;

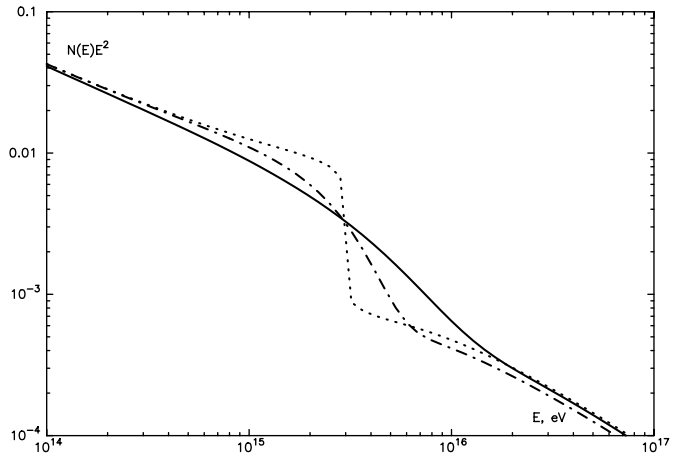

Fig. 6. Spectral energy distributions (in arbitrary units) of the CR protons in the Galaxy for different cut-off forms: exponential (solid curve), $\propto\exp(-p^2/p_{\max}^2)$ (dash-dotted curve) and the sharp cut-off (dotted curve).

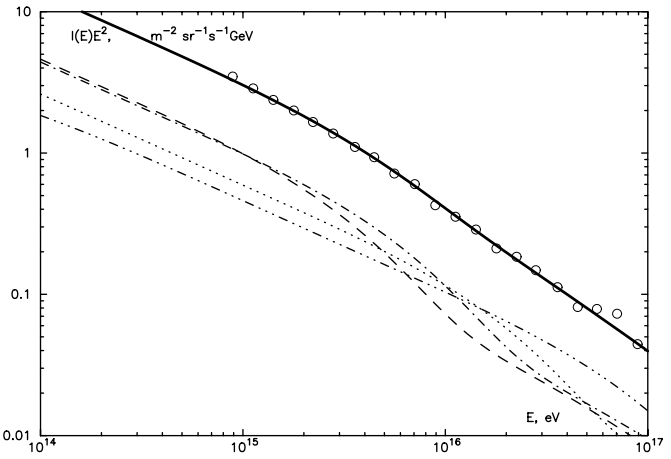

Fig. 7. Calculated differential spectral flux $I(E)$ (in units of $\mathrm{m^{-2}\ sr^{-1}\ s^{-1}\ GeV^{-1}}$) of the CR protons (dashed curve), helium nuclei (dash-dotted curve), carbon (dotted curve), iron (dash-dot-dotted curve), all-particle (solid curve) in the Galaxy for the exponential cut-off, and the all-particle spectral flux observed by the KASCADE collaboration (empty circles). The chemical composition has been fixed at $E = 9 \times 10^{14}$ eV from Fig. 5 of Kampert et al. (2001). The data for the all-particle spectrum are also taken from Kampert et al. (2001).

Zirakashvili et al. 1996; Ptuskin et al. 1997). We believe that now a convincing physical picture for the Galactic halo, including gas, magnetic field and CRs exists. CR sources in the Galactic disk produce energetic particles – the Disk-CRs – which mainly drive the Galactic Wind flow with its frozen-in magnetic field. CR streaming along magnetic field lines excites Alfvén waves. Nonlinear damping of these waves results in gas heating up to temperatures of the order of a million degrees in the galactic Halo (cf. Zirakashvili et al. 1996). The balance of wave damping and wave excitation determines the level of Alfvénic turbulence which in turn determines the scattering efficiency and hence the diffusion of the CR particles. The CR spectrum observed up to the maximum particle energies resulting from the source spectra produced by acceleration in Supernova Remnants (presumably $E < E_{\rm knee} \sim 3 \times 10^{15}\, Z$ eV) can be fully explained in this self-consistent nonlinear model. For the explanation of the higher energy part of the spectrum we propose a reacceleration mechanism in the Galactic Wind flow for the most energetic particles from the disk. The lower energy CRs are produced more effectively in the Galactic spiral arms and therefore should drive a more powerful wind above the arms. The interaction of these fast streams with the slow streams from the interarm regions can result in shock formation at large distances from the Galaxy. These shocks are similar to the Corotating Interaction Region shocks of the outer Solar Wind. CR particles from the disk can be reaccelerated on these shocks by a diffusive shock acceleration mechanism to generate the Wind-CRs. The discussion of the very simple results shown in Figs. 5 and 7 allows us to conclude that the observations do not contradict the idea.

We should underline the very important role of the termination shock. The expected strong turbulence associated with it results in an energy independent loss of particles with energies smaller than about $10^{17}\, Z$ eV. In practice this is the maximum energy for the model considered. Higher energy particles require accelerating sources outside the termination shock. Alternatively they may be the ubiquitous result of the decay of superheavy particles left over from the early Universe.

Appendix A: Influence of the termination shock on high energy particles

We consider a spherically symmetric wind flow with velocity u. Beyond the termination shock at radius $R_{\rm s}$ the diffusion coefficient fulfills the inequality $D \ll uR_{\rm s}$ if the turbulence level is sufficiently high. Interior to this dissipation layer we have an interplay between diffusion and advection. The radius of the diffusion-advection boundary $R_{\rm da}(p)$ is determined by the condition $D(p, R_{\rm da}) \sim uR_{\rm da}$. Inside this zone advection is small and will be neglected. The solution of the pure diffusion equation between r_0 and $R_{\rm da}$ is

$$N(p,r) = N_0 + (N_{\rm da} - N_0) \int_{r_0}^{r} \frac{{\rm d}r'}{r'^2 D(p,r')} \Bigg/ \int_{r_0}^{R_{\rm da}} \frac{{\rm d}r'}{r'^2 D(p,r')} \cdot \quad \text{(A.1)}$$

Here $N_{\rm da}$ and N_0 are the CR distribution functions at the distances $R_{\rm da}$ and r_0 (Galactic disk radius), respectively. The boundary condition at $r = r_0$ and the continuity condition at $r = R_{\rm da}$ are:

$$D \frac{\partial N}{\partial r}\bigg|_{r=r_0} = -Q(p) \quad \text{(A.2)}$$

and

$$D \frac{\partial N}{\partial r}\bigg|_{r=R_{\rm da}} = u \frac{p}{3} \frac{\partial N}{\partial p}. \quad \text{(A.3)}$$

As a result

$$N_{\rm da} = 3 \frac{r_0^2}{u} \int_p^{\infty} \frac{{\rm d}p'}{p'} \frac{Q(p')}{R_{\rm da}^2(p')}, \quad \text{(A.4)}$$

$$N_0 = 3\frac{r_0^2}{u}\int\limits_p^\infty \frac{\mathrm{d}p'}{p'}\frac{Q(p')}{R_{\rm da}^2(p')} + r_0^2 Q(p)\int\limits_{r_0}^{R_{\rm da}(p)} \frac{\mathrm{d}r'}{r'^2 D(p,r')}. \qquad (A.5)$$

If the diffusion coefficient is inversely proportional to r^2 (this is the case in the self-consistent model of Ptuskin et al. (1997) because of the factor $\cos^2\alpha$), the integral over r' in the last expression is determined by the upper limit and is comparable with the first term. A source momentum spectrum with index 4.0 and a diffusion coefficient proportional to p give the value $14/3 \simeq 4.67$ for the index of the observable spectrum.

For larger energies the radius $R_{\rm da}(p)$ is comparable with $R_{\rm s}$ and limited by it. Therefore, for these energies

$$N_0 = 3\frac{r_0^2}{uR_{\rm s}^2}\int\limits_p^\infty \frac{\mathrm{d}p'}{p'}Q(p') + r_0^2 Q(p)\int\limits_{r_0}^{R_{\rm s}} \frac{\mathrm{d}r'}{r'^2 D(p,r')}. \qquad (A.6)$$

This means that the momentum spectrum becomes hard like the source spectrum.

If, for example, the diffusion coefficient was independent of r, then the second term can dominate the first term for $uR_{\rm s} \ll D \ll uR_{\rm s}^2/r_0$ in the last equation. But in this case the spectrum inside the Galaxy would be determined by diffusion only and one should take for example a value of 4.0 for the source index and the diffusion coefficient proportional to $p^{0.67}$ in order to reproduce the observable spectrum. It becomes again hard for high enough energies $D \gg uR_{\rm s}^2/r_0$.

Appendix B: CR acceleration by the SIR shock system

Let us investigate the diffusive acceleration by a periodic shock wave. Let the velocity profile be a continuous function $u(x)$ for $0 < x < L$ where L is period of the wave. Shocks are located at $x = 0$, $x = L$, $x = 2L$, etc. At each shock the flow velocity drops from the value $u_1 = u(L-0)$ to the value $u_2 = u(0+0)$.

We shall consider the case of a small diffusion coefficient, characterized by the inequality $D \ll uL$. In this case the particle is convected by the flow from one shock to the neighboring one, where it is diffusively accelerated. Subsequently it is convected to the next shock where it is accelerated again, etc.

Let $N(p)$ be the particle distribution function in momentum p. It is normalized as $\int 4\pi p^2 \mathrm{d}p N(p) = n$, where n is the particle number density. Near the shock particles are accelerated and $N(p)$ changes correspondingly. The relation between upstream and downstream distributions is given by diffusive acceleration theory (e.g. Blandford & Ostriker 1980)

$$N_{\rm down}(p) = \gamma_{\rm s}\int\limits_0^p \frac{\mathrm{d}p'}{p'}\left(\frac{p'}{p}\right)^{\gamma_{\rm s}} N_{\rm up}(p'), \qquad (B.1)$$

where $\gamma_{\rm s} = 3\sigma_{\rm s}/(\sigma_{\rm s}-1)$ is the power law index of particles accelerated by a single shock with compression ratio $\sigma_{\rm s} = u_1/u_2$. For our purposes it is more convenient to use the Mellin transform $F(s) = \int\limits_0^\infty \mathrm{d}p p^{s-1} N(p)$. Then $F_{\rm down}(s) = F_{\rm up}(s)/(1 - s/\gamma_{\rm s})$. Between the shocks a particle loses energy adiabatically. The distribution function $N(p)$ then transforms into $N(p\sigma_{\rm s}^{1/3})$. For the Mellin transform such a transformation reduces to a multiplication with $\sigma_{\rm s}^{-s/3}$. Hence, after n acceleration cycles the Mellin transform of the distribution function is given by

$$\begin{aligned} F_n(s) &= F_0(s)\sigma_{\rm s}^{-sn/3}/(1 - s/\gamma_{\rm s})^n \\ &= F_0(s)\exp\left(-n\left(\frac{s}{3}\ln\sigma_{\rm s} + \ln(1 - s/\gamma_{\rm s})\right)\right). \end{aligned} \qquad (B.2)$$

One can check that this does not depend on the initial position of the particle. It can be near the shock or somewhere between the shocks. Let us now introduce the cycle duration $T = \int\limits_0^L \mathrm{d}x/u(x)$. Then, at the time $t = nT$, the function $F_n(s)$ can be found as the solution of the equation

$$\frac{\partial F(s)}{\partial t} = -\frac{F(s)}{T}\left(\frac{s}{3}\ln\sigma_{\rm s} + \ln(1 - s/\gamma_{\rm s})\right) \qquad (B.3)$$

with the initial condition $F(s)|_{t=0} = F_0(s)$. This equation for the Mellin transform $F(s)$ corresponds to the following equation for the distribution function $N(p)$:

$$\frac{\partial N}{\partial t} = \frac{1}{T}\left[\frac{p}{3}\frac{\partial N}{\partial p}\ln\sigma_{\rm s} - \int\limits_0^p \frac{\mathrm{d}p'}{p'}\left(\frac{p'}{p}\right)^{\gamma_{\rm s}} \frac{N(p') - N(p)}{\ln(p'/p)}\right]. \qquad (B.4)$$

It is simple to verify that the Mellin transform of this equation gives Eq. (B.3). In this procedure the value of integral

$$\int\limits_0^\infty \frac{\mathrm{d}y}{y}\left(\mathrm{e}^{-ay} - \mathrm{e}^{-by}\right) = \ln(b/a), \quad a > 0, b > 0$$

should be used.

It is important that the adiabatic energy losses described by the first term in square brackets of Eq. (B.4) enter this equation additively. This derivation is also valid in the presence of energy independent additional energy losses or escape of particles. The corresponding terms should be added to the right-hand side of Eq. (B.4).

For weak shocks $\sigma_{\rm s} - 1 \ll 1$ the operator on the rhs of Eq. (B.4) is reduced to diffusion in momentum space. The corresponding diffusion coefficient is given by:

$$D_{pp} = \frac{p^2}{18}\frac{(\Delta u)^2}{v_{\rm s}L}, \qquad (B.5)$$

where $v_{\rm s}$ is the shock velocity and $\Delta u = u_1 - u_2$ is the velocity jump at the shock.

In the case of a saw-tooth wave velocity profile

$$u(x) = u_2 + (u_1 - u_2)\frac{x}{L} \qquad (B.6)$$

$T = L\ln\sigma_{\rm s}/\Delta u$, and the rhs of Eq. (B.4) reduces to the last term in Eq. (17) of the main text.

Acknowledgements. The work of V.N.Z. was done during his visit at the Max-Planck-Institut für Kernphysik in Heidelberg under the auspices of the Sonderforschungsbereich 328 and was also supported by the Russian Foundation of Basic Researches grant 01-02-17460. We thank an anonymous referee for many important comments.

References

Achterberg, A. 1990, A&A, 231, 251
Allen, C., & Santillán, A. 1991, Rev. Mex. Astron. Astrofis., 22, 255
Antoni, T., Apel, W. D., Badea, F., et al. 2002, Astropart. Phys., 16, 245
Axford, W. I. 1994, ApJS, 90, 937
Bell, R. A., & Lucek, S. G. 2001, MNRAS, 321, 433
Berezinsky, V. S., & Ptuskin, V. S. 1988, Sov. Astron. Lett., 14, 304
Berezhko, E. G., & Krymsky, G. F. 1983, Proc. 18th ICRC (Bangalore), 2, 255
Bhattacharjee, P., & Sigl, G. 2000, Phys. Rep., 327, 109
Biermann, P. L. 1993, A&A, 271, 649
Blandford, R. D., & Ostriker, J. P. 1980, ApJ, 237, 793
Breitschwerdt, D., Völk, H. J., & McKenzie, J. F. 1991, A&A, 245, 79
Breitschwerdt, D., McKenzie, J. F., & Völk, H. J. 1993, A&A, 269, 54
Breitschwerdt, D., Dogiel, V. A., & Völk, H. J. 2002, A&A, 385, 216
Bykov, A. M., & Toptygin, I. N. 1988, Bull. Acad. Sci. USSR, 52, 1
Cranmer, S. R., & Owocki, S. P. 1996, ApJ, 462, 469
Drury, L. O'C., & Völk, H. J. 1981, ApJ, 248, 344
Fernández, D., Figueras, F., & Torra, J. 2001, A&A, 372, 833
Fisk, L. A., & Lee, M. A. 1980, ApJ, 237, 620
Forslund, D. W., & Freiberg, J. P. 1971, Phys. Rev. Lett., 27, 1189
Han, J. L., & Qiao, G. J. 1994, A&A, 288, 759
Hillas, A. M. 1984, ARA&A, 22, 425
Ip, W. H., & Axford, W. I. 1991, AIP Conf. Proc., 264, 400
Ipavich, F. M. 1975, ApJ, 196, 107
Jokipii, J. R., & Morfill, G. 1985, ApJ, 290, L1
Jokipii, J. R., & Morfill, G. 1987, ApJ, 312, 170
Jokipii, J. R. 1987, ApJ, 313, 842
Kampert, K.-H., Antoni, T., Apel, W. D., et al. 2001, Proc. 27th ICRC (Hamburg), 240
Klepach, E. G., Ptuskin, V. S., & Zirakashvili, V. N. 2000, Astropart. Phys., 13, 161
Lagage, P. O., & Cesarsky, C. J. 1983, A&A, 125, 249
Lépin, J. R., & Amaral, L. H. 1997, MNRAS, 286, 887
Lépin, J. R., Mishurov, Y. N., & Dedikov, S. Y. 2001, ApJ, 546, 234
Lin, C. C., & Shu, F. H. 1964, ApJ, 140, 646
Lin, C. C., Yuan, C., & Shu, F. H. 1969, ApJ, 155, 721
Lucek, S. G., & Bell, A. R. 2000, MNRAS, 314, 65
Melrose, D. B., & Pope, M. H. 1993, Proc. Astron. Soc. Austr., 10, 222
Parker, E. N. 1958, ApJ, 128, 664
Ptuskin, V. S., Völk, H. J., Zirakashvili, V. N., & Breitschwerdt, D. 1997, A&A, 321, 434
Roth, M., Ulrich, H., Antoni, T., et al. 2003, Proc. 27th ICRC (Tsukuba), 139
Sagdeev, R. Z. 1966, in Reviews of Plasma Physics, ed. M. A. Leontovich (New York: Consultants Bureau)
Sommers, P. 2001, Proc. 27th ICRC (Hamburg), Invited, Rapporteur, and Highlight papers, 170
Spruit, H. C. 1988, A&A, 194, 319
Völk, H. J. 1984, in High Energy Astrophysics, Proc. 19th Rencontre de Moriond, ed. Tran Than Van (Éditions Frontières, Gif-sur-Yvette), 281
Völk, H. J. 1987, Proc. 20th ICRC (Moscow), 7, 157
Völk, H. J., & Biermann, P. L. 1988, ApJ, 333, L65
Völk, H. J., Berezhko, E. G., Ksenofontov, L. T., & Rowell, G. P. 2002, A&A, 396, 649
Zirakashvili, V. N., Breitschwerdt, D., Ptuskin, V. S., & Völk, H. J. 1996, A&A, 311, 113
Zirakashvili, V. N., Ptuskin, V. S., & Völk, H. J. 2001, Proc. 27th ICRC (Hamburg), 1827